ACS Energy LETTERS

http://pubs.acs.org/journal/aelccp

FOCUS REVIEW

Development of InP Quantum Dot-Based Light-Emitting Diodes

Zhenghui Wu, Pai Liu, Wenda Zhang, Kai Wang, and Xiao Wei Sun*

Cite This: *ACS Energy Lett.* 2020, 5, 1095−1106

Read Online

ACCESS | Metrics & More | Article Recommendations

ABSTRACT: High-performance quantum dot light-emitting diodes (QLEDs) are being considered as a next-generation technology for energy efficient solid-state lighting and displays. InP QLEDs are the most promising alternative to the toxic CdSe QLEDs. Unlike the problems of poor hole injection in CdSe-based QLEDs, highly delocalized electrons and parasitic emissions are serious problems in green-emitting InP QLEDs. The loss mechanism and device physics in InP QLEDs have not been sufficiently studied since the first report of InP QLED in 2011. This Focus Review summarizes the recent efforts on improving the performance of InP QLEDs from the perspectives of core/shell structures to optimization of carrier transport layers. It is our intention to conduct a review as well as clarify some previous misunderstandings regarding the device physics in InP QLEDs and to provide some insights for the possible solutions to the challenging problems in InP QLEDs.

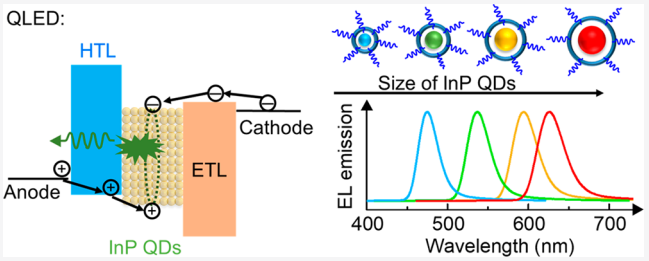

One of the most impressive successes in the market of display products was the application of active matrix (AM) organic light-emitting diodes (OLEDs) in cell phones. However, there are some intrinsic drawbacks in OLEDs. Organic emissive materials are intrinsically less stable and less bright than inorganic materials. This suggests they are difficult to apply in large TV screens or outdoor screens, which are expected to be used for >5 years. The road map to better display and lighting products includes (a) improving the product parameters of traditional light-emitting diodes (LEDs) based on classical bulk semiconductors[1,2] and (b) exploration of new classes of light-emitting materials, such as metal halide perovskites and quantum dots (QDs).[3,4] Quantum dots (QDs) are inorganic semiconductor nanoparticles with excellent stability, whose optical and electrical properties are strongly dependent on their particle sizes and chemical compositions.[5−10] The development of quantum dot light-emitting diodes (QLEDs), namely, electrically driven luminescent (EL) devices, provides a possible way to maximize the advantages of QDs, such as energy savings, ultrawide color gamut, and flexible processability.[11] Considering more than 20% of the energy used in the world was consumed by lighting alone, QLEDs are the most promising candidates for next-generation energy-efficient displays and solid-state lighting.[12−15] The most studied QDs are cadmium selenide (CdSe) based, including CdSe/ZnS,[16,17] CdSe/ZnSe,[18,19] and CdSe/CdS/ZnS or CdSe/ZnSe/ZnS.[20−22] Because of the development of QDs with finely controlled core/shell structure, high-performance QLEDs with external quantum efficiency (EQE) of over 20% have been realized.[23−26] However, those achievements were all based on the heavy metal-containing CdSe, which can cause serious chronic diseases and cancer.[27,28] There is increasing interest in Cd-free QDs in the scientific community. Though there is sufficient physical understanding of the device structures and loss mechanisms in Cd-based QLEDs, as summarized in Chen, Guan, and Tang's review,[29] the physics and loss mechanisms may be very different if a new class of QDs is used in QLEDs. During the recent decades, the most studied Cd-free QDs included InP,[30,31] ZnSe,[32,33] $CuInS_2$,[34,35] and group IV QD (carbon dots and silicon QD).[36,37] Because of the large band gap, ZnSe QDs can emit only violet-blue light.[38,39] On the other hand, $CuInS_2$ and type IV-based QDs usually show broad emission spectra because of the emission from trap states or impurities,[40−42] which make them not suitable for displays. With 1.35 eV bulk band gap and 10 nm excitonic Bohr radius, InP QDs can be tuned to emit blue, green, and red light,[43,44] and their emission character is also competitive. Therefore, InP QLEDs are regarded as the most promising alternative Cd-free QLEDs for display and lighting applications.

Received: December 27, 2019
Accepted: March 5, 2020
Published: March 5, 2020

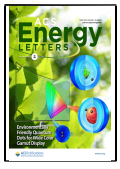

https://dx.doi.org/10.1021/acsenergylett.9b02824
ACS Energy Lett. 2020, 5, 1095−1106

However, the progress of InP QLEDs still lags far behind that of the state-of-the-art Cd-based QLEDs. The efforts to improve the performance of InP QDs have continued for more than 20 years. The most recent achievements regarding InP QLEDs reported in journal articles were represented by 6.2% EQE in the green region[45] and 21.4% EQE in the red region.[46] Early works mainly focused on improving the synthetic routes to obtain high quantum yield of QDs in solution. More details on understanding the synthesis of high-quality InP QDs are reviewed later in this work. On the other hand, the device studies of InP QLEDs were not reported until 2011.[47] Since 2011, the reported high-performance InP QLEDs were mainly due to high-quality crystallization in InP QDs with minimal traps and precise control of shell growth.[45,48] Nevertheless, more studies on device physics are needed to achieve high-performance InP QLEDs. A QLED usually consists of multiple thin films including anode, hole injection layer (HIL), hole transport layer (HTL), QD emissive layer, electron transport/injection layer (ETL/EIL), and cathode.[49−51] There are many excellent reviews on the physical understanding of devices and materials in Cd-based QLEDs.[11,52−54] However, physical studies of InP QLEDs were not particularly reviewed in the literature. In most works on InP QLEDs, the HTL and ETL were selected based on previous experience regarding Cd-based QLEDs without changing parameters. However, the electronic properties of InP QDs are distinct from those of Cd-based QDs. The different loss mechanisms and challenges between InP and Cd-based working QLEDs have not drawn enough attention in the community. A later discussion in this Focus Review focuses on the understanding of device structures of InP QLEDs. We also provide useful guidelines for addressing the challenges specific to InP QLEDs.

Synthesis of luminescent InP QDs dates back to the 1990s.[30,31,55] In the early days, surface ligands were directly bonded to InP QDs without a shell.[43,56,57] The InP QDs reported in the above references usually showed broad emission, asymmetry, and sometimes shoulders in their photoluminescence (PL) spectra. These problems were closely related to the surface traps, where mainly nonradiative recombination happened and PL emission was largely suppressed. The broad emission sometimes also resulted from the broad distribution of particle size. On the basis of a great deal of previous experience, InP QDs showing symmetric and single-peak PL spectra were first synthesized by using a noncoordinating solvent and strictly controlled reaction conditions in 2002.[43] The noncoordinating solvent, the chain length of certain ligands, the ratio of metal atoms to ligands, and reaction environment were all critical parameters to address the problems of broad emissions, long tail, or shoulders in the PL spectra. However, the PL quantum yield (PLQY) values of all of the above InP QDs in solution were still less than 10%.

In 2000, the first report of a core/shell structure in InP QDs appeared.[58] A compound semiconductor $ZnCdSe_2$ with excellent lattice match with InP was chosen as the shell to ensure high-quality epitaxial growth. Because of the perfect lattice match, the shell thickness can be easily grown up to 5 nm. However, it was found that the electrons were delocalized over the whole nanocrystal, resulting in less than 10% PLQY. The poor electron confinement was due to the small offset between the conduction band minima (CBM) of InP and $ZnCdSe_2$. Later, like CdSe QD, the large band gap semiconductor ZnS was used as the shell.[59] However, because of the large lattice mismatch between InP and ZnS, as shown in Figure 1a, the surface of the InP core was not fully covered by

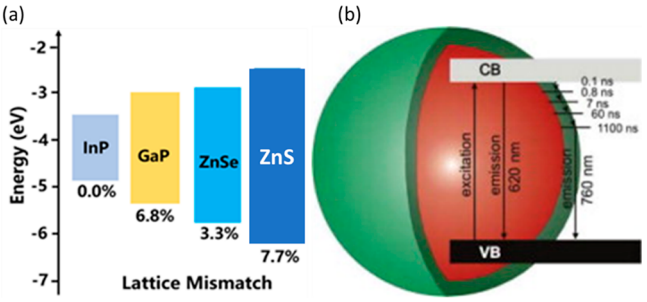

Figure 1. (a) Lattice mismatches between InP and other semiconductors that were usually used as shells. (b) Illustration of the emission from trap sites in InP QDs. Reprinted with permission from ref 64. Copyright 2010 Elsevier.

ZnS. Surprisingly, the InP/ZnS without full coverage of shell showed record high PLQY (20%). The surprising result was due to the electron confinement in InP/ZnS QDs. The comparison between the results in refs58 and 59 suggested more efforts should be devoted to the growth of a high-quality ZnS or ZnSe shell, rather than exploration of new shell materials with excellent lattice match with the InP core. After years of efforts, a new synthetic method using activation reagents and low-temperature processing (<190 °C) was developed to synthesize InP/ZnS core/shell QDs with tunable particle sizes and emission peaks in the range of 480−750 nm.[60] The new synthetic method allowed better control over the particle size. The PLQY also increased to the new high of 40%. In 2008, rapid processes to grow both the core and ZnS shell were reported.[61] The growth of the InP core took only 10 min, while the shelling process took only 20 min. Because of the fast synthesis process, QDs with uniform size were achieved without a size selection process. The PLQY of the InP/ZnS core/shell QDs was 60%, which was the highest at that time. In 2008, Li reported a synthesis of green InP/ZnS QDs with 70% PLQY, and there was no precursor injection in the synthesis process.[44] Ryu's work in 2009 offered important insight into the important role of zinc acetate in surface etching and surface formation.[62] On the basis of this understanding, blue InP/ZnS QDs with PL emission peak at 475 nm and full width at half maximum (FWHM) of 39 nm were achieved by a subtle balance between the surface etching and shell growth.[63] This was the shortest wavelength of the emission peak of InP/ZnS QDs at the reporting time. On the other hand, the studies on the PL kinetic profiles revealed that the poor PL in InP QDs mainly resulted from the trapped electrons at the InP surface.[64] The large lattice mismatch between InP and ZnS was responsible for the large amount of trap sites. As shown in Figure 1b, part of the trapped electrons radiatively recombined with holes in the valence band and emitted light with red-shifted or long-tail spectrum, while most of the trapped electrons were lost through nonradiative processes. This may be the reason that the above InP/ZnS QDs with high PLQY were not successfully applied in fabricating QLEDs as expected, because traps may have complex impacts on the electro-injection of carriers. Novel synthetic approaches should be developed to reduce the electron traps at the core−shell interface so that the luminescence emission mainly results from

https://dx.doi.org/10.1021/acsenergylett.9b02824
ACS Energy Lett. 2020, 5, 1095−1106

Novel synthetic approaches should be developed to reduce the electron traps at the core−shell interface so that the luminescence emission mainly results from the recombination between electrons in the conduction band and holes in the valence band.

the recombination between electrons in the conduction band and holes in the valence band.

In 2010, the In(Zn)P/ZnS and InPZnS/ZnS QDs with alloy cores were found to confine electrons better,[65,66] which inspired the idea of double-shell QDs, or core/shell/shell QDs. Because of the excellent photo- and air-stability of ZnS and its large band offset with InP, ZnS is the most desired material for the outermost shell of InP QDs. As shown in Figure 1a, the two promising candidates for the intermediate shell are GaP and ZnSe. The InP/ZnSe:ZnS QD with composition gradient shell was reported in 2011.[47] The ZnSe composition tended to be closer to the InP core. This was the first time to get >1 nm ZnS shell in InP-based QDs with excellent confinement of excitons. It was also the first time to successfully fabricate a working QLED based on InP QDs. In 2012, synthesis of InP/GaP/ZnS QDs with maximum PLQY of 85% and excellent photochemical stability was reported.[67] In 2016, the process of the synthesis of InP/GaP/ZnS QDs was improved to be more efficient, and the resulted InP/GaP/ZnS QDs show PLQY of 90%, fwhm of 40 nm.[68] In recent years, there were another several publications reporting InP/shell/shell QDs. These works are carefully reviewed and explained in the next section, because they all reported working EL devices.

The conventional and inverted device structures of typical QLEDs were shown in Figure 2. In the conventional structure,

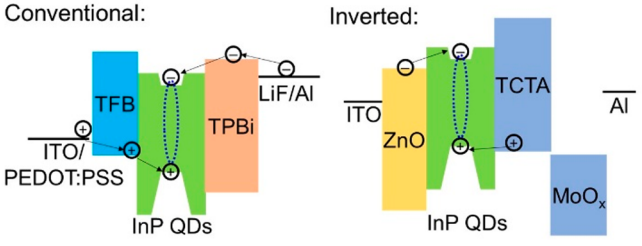

Figure 2. Typical device structures of conventional and inverted InP-based QLEDs.

PEDOT:PSS is hole injection layer, with full name of poly(3,4-ethylenedioxythiophene) polystyrenesulfonate. Poly(9,9-dioctylfluorene-*alt*-N-(4-s-butylphenyl)-diphenylamine) (TFB) is a commonly used HTL material. 2,2′,2″-(1,3,5-Benzinetriyl)-tris(1-phenyl-1-H-benzimidazole) (TPBi) is a commonly used ETL. LiF is an ultrathin layer for electron injection. In the inverted structure, TCTA is a typical hole transport layer, with full name of 4,4′,4″-Tris(carbazol-9-yl)triphenylamine. MoO_x is used for hole injection. These HTL/ETL may be replaced by semiconductors with similar energy levels and hole/electron mobilities. Since the first reported InP QLED in 2011,[47] a lot of efforts were devoted to improving the device performance of InP QLED. These efforts included 1) improve the exciton confinement and radiative recombination through better control of shell growth; 2) optimize the electron transport layer and the hole transport layer. In the next three sections, these efforts are thoroughly discussed, based on the facts reported in previous publications and our unpublished experimental data. The discussions intend to gain better understanding of the loss mechanism specific to InP QLED, and to provide helpful guidelines for further improvement of InP QLED in future.

As explained in Section 2, ZnS was highly desired for the outermost shell. Atoms from III and V groups are easily doped into II−VI atoms including Zn, S, O, Se, and vice versa.[69,70] The interdoping between InP and ZnS and oxidation of InP inevitably generate a lot of surface traps, which induce significant nonradiative loss, such as Förster resonant energy transfer (FRET) and Auger recombination (AR).[71−73] Growth of high-quality shell without interface or surface traps are essential to achieve high performance InP QLED. In the first reported InP QLED, a thick ZnSeS shell with uniform gradient of composition was wrapped over the InP core.[47] ZnSe preferred to be closer to the InP core, so ZnSe acted as a lattice adaptor to alleviate the lattice strain on the surface of InP, resulting in suppression of surface traps in InP QDs. But the EQE was only <0.1%. This may be due to the poor electron confinement. The offset between the CBMs of InP and ZnSeS (~0.2 eV) was too small, so that the wave functions of electrons became delocalized and extended to the shell.[74,75] Shortly later in 2012, InP/ZnS QDs was used to fabricate QLED with a structure of ITO/PEDOT:PSS/Poly-TPD/InP QDs/TPBi/LiF/Al.[76] Poly-TPD was the HTL with full name of Poly[N,N′-bis(4-butylphenyl)-N,N′-bisphenylbenzidine]. The emission spectrum of the above LED covered the full visible spectral range, with three peaks including emissions from Poly-TPD and InP QDs. Thus, the above InP QLED was suitable only for white lighting applications, but not displays. Because of the large lattice mismatch, the ZnS shell was not uniform and its electron confinement effect was rather poor. This was responsible for the emission from transport layers, i.e. parasitic emissions. The illustration of parasitic emission was shown in Figure 3a. The electrons in the InP QD layer were highly delocalized and easily transferred among the QDs and also between different layers. Figure 3b shows a typical EL emission spectrum with parasitic emission. Almost at the same time, InP/ZnSeS QDs were used to replace InP/ZnS QDs by the same group.[77] Compared to the first reported InP/ZnSeS QLEDs, the temperature control during the process of shell

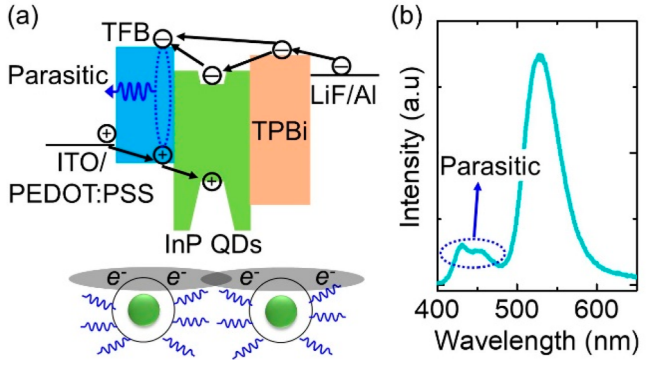

Figure 3. (a) Illustration of the parasitic emission in InP QLED. (b) Typical EL emission spectrum of InP QLED with parasitic emission.

https://dx.doi.org/10.1021/acsenergylett.9b02824
ACS Energy Lett. 2020, 5, 1095−1106

growth was improved, so that the EQE of the green QLED based on InP/ZnSeS was improved by 3 fold, i.e., EQE = 0.26%. However, the parasitic emission from Poly-TPD was still significant. In 2013, the distribution of chemical composition in the shell of InP/ZnSeS QDs was improved so that the electrons were better confined, and the EQE was boosted up to 3.4%.[78] In this work, the uniform alloy shell kept a balance between alleviation of lattice strain and the high enough band offset. This work also showed that larger sized QDs with thicker ZnSeS shell showed better performance in QLED and suppressed parasitic emission, though its PLQY was lower.

Within the last three years, more complicated synthesis processes were developed to synthesize InP QDs with large particle size and thick shells. Red InP QLEDs with emission peak beyond 600 nm had not been reported until 2016, because of the challenges in increasing the QD size and compromising fwhm. The red InP QLED with 2.5% EQE was achieved by 7.2 nm InP QDs with double-shell structure InP/ZnSeS/ZnS.[79] A delicate procedure was used to grow the alloy ZnSeS intermediate shell by alternately injecting anionic and cationic shell precursors at designated temperatures. ZnS was grown at the outer shell to get large-sized QDs. Because of the large size and thick shell, the parasitic emission from the charge transport layer was easily suppressed without too much effort to optimize the transport layer. In 2018, prestine ZnSe, rather than an alloy intermediate shell, was grown in InP/ZnSe/ZnS QDs to more efficiently alleviate the lattice strain, so that extremely large InP QDs (15 nm) with an ultrathick ZnS outer shell became possible.[80] The wave functions of the electrons and holes were deeply extended into the ZnSe layer, resulting in a large red shift (0.42 eV) of the emission peak compared to the bare InP core. Therefore, the InP/ZnSe/ZnS QDs in this work were actually double-core QDs. The InP/ZnSe/ZnS QDs achieved record high EQE (6.6%) in red InP QLEDs and very narrow emission peak (fwhm = 40 nm) without parasitic emission. More recently, in 2019, a more complicated shell structure of InP/GaP/ZnS/ZnS was introduced to achieve record high EQE (6.2%) in green InP QLEDs.[45] The growth of a very thick ZnS outer shell succeeded because of the long growth time and timely replenishment of the ZnS precursor. The very thick ZnS outer shell suppressed the nonradiative FRET processes. However, this green InP QLED showed significant parasitic emission and very broad emission peak (fwhm > 70 nm). With a smaller InP core, green InP QLEDs more easily suffered from parasitic emission compared to red InP QLEDs. InP/GaP/ZnS QDs were actually reported two times several years ago.[67,68] However, fabrication of fully functioning InP QLEDs was not successful previously. In addition to the thickness of the shells, better control of the crystallization and chemical composition in the shells was also important for the electroluminescence. Also in 2019, a simpler structure of InP/ZnSe/ZnS but with a more delicate control of synthetic process was developed, achieving 12.2% EQE in red InP QLEDs.[48] The stoichiometry controlled InP/ZnSe/ZnS showed nearly unit PLQY, excellent ambient stability, and suppressed PL blinking. The key of stoichiometry-controlled synthesis was to ensure simultaneously stoichiometry of In and P in the core and prevent the incorporation of In atoms into the shells. The shell growth was also stoichiometry controlled to reduce the interfacial and surface traps. Because of the delicate control of both core and shells, excellent quantum confinement was achieved by QDs with only 7.2 nm diameter. The most recent record high EQE in red InP QLED was 21.4%.[46] The ZnSe shell was grown simultaneously by injecting a Se precursor containing hydrofluoric acid to prevent reoxidation of InP core surface. The reaction temperature was raised to a record high, i.e., 340 °C, to facilitate a kinetically controlled reaction on a random facet, so that the shell was more uniform and the InP/ZnSe/ZnS QD morphology was more spherical.

As shown in Figure 4, many HTLs and ETLs with different energy levels were used in QLEDs. The full names of some

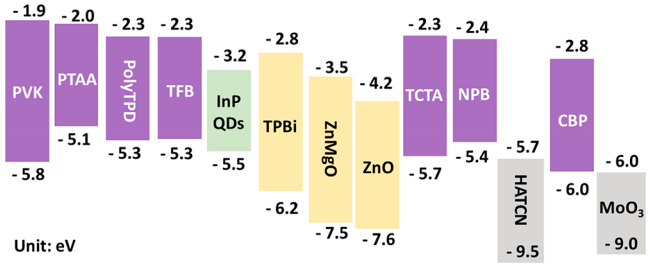

Figure 4. Energy levels of the commonly used HTL (purple), ETL (yellow), HIL (gray), and green-emitting InP QDs (green).

organic transport/injection layers are summarized here: poly(9-vinylcarbazole) (PVK), poly[bis(4-phenyl)(2,4,6-trimethylphenyl)amine] (PTAA), *N*,*N*′-Di(1-naphthyl)-*N*,*N*′-diphenyl-(1,1′-biphenyl)-4,4′-diamine (NPB), 1,4,5,8,9,11-hexaazatriphenylenehexacarbonitrile (HATCN), and 4,4′-Bis-(9-carbazolyl)-1,1′-biphenyl (CBP).

Most of the previous publications[45,78−80] reported CBMs and valence band maxima (VBMs) of InP/shell/shell QDs ranging from −3.0 to −3.7 eV and −5.1 to −5.7 eV, respectively, while the CBMs and VBMs of CdSe-based QDs were usually deeper than −4 and −6.0 eV, respectively.[81] As shown in Figure 5, the structure of ITO/PEDOT:PSS/Poly-TPD/InP QDs/TPBi/LiF/Al was first applied in InP-based QLEDs.[47,77] Considering the well-known principle that the hole/electron injection levels should match with the VBM/CBM of the QD layer, using Poly-TPD as HTL and TPBi as ETL was reasonable.[82,83] However, both of the works using this device structure did not result in high efficiency; instead, significant parasitic emission from Poly-TPD was observed, as shown in Figure 5. The ultimate solution to the parasitic

> The ultimate solution to the parasitic emission is to synthesize InP QDs with excellent electron confinement, which is especially challenging in green-emitting InP QDs. However, wise design of device structure can also address this problem and enhance the performance of QLEDs.

emission is to synthesize InP QDs with excellent electron confinement, which is especially challenging in green-emitting InP QDs. However, wise design of device structure can also address this problem and enhance the performance of QLEDs. The following discussion about the suppression of parasitic emission mainly focuses on green-emitting InP QLEDs.

https://dx.doi.org/10.1021/acsenergylett.9b02824
ACS Energy Lett. 2020, 5, 1095−1106

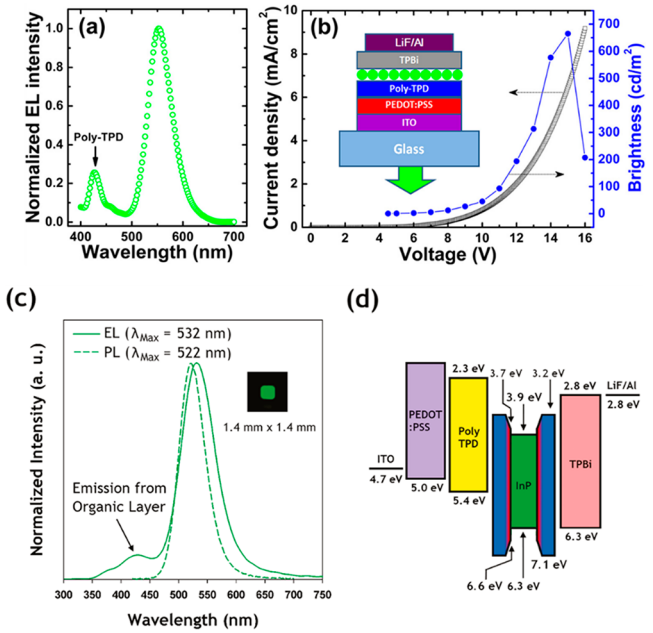

Figure 5. (a) EL emission spectrum with parasitic emission of InP-based QLED studied in ref 77. (b) The device structure and voltage−current−luminance (*J*−*V*−*L*) characteristics of the QLED studied in in ref 77. Reprinted with permission from ref 77. Copyright 2012 AIP Publishing. (c) The EL emission spectrum with parasitic emission of InP-based QLED studied in ref 47. (d) The device structure of the QLED studied in ref 47. Reprinted from ref 47. Copyright 2011 American Chemical Society.

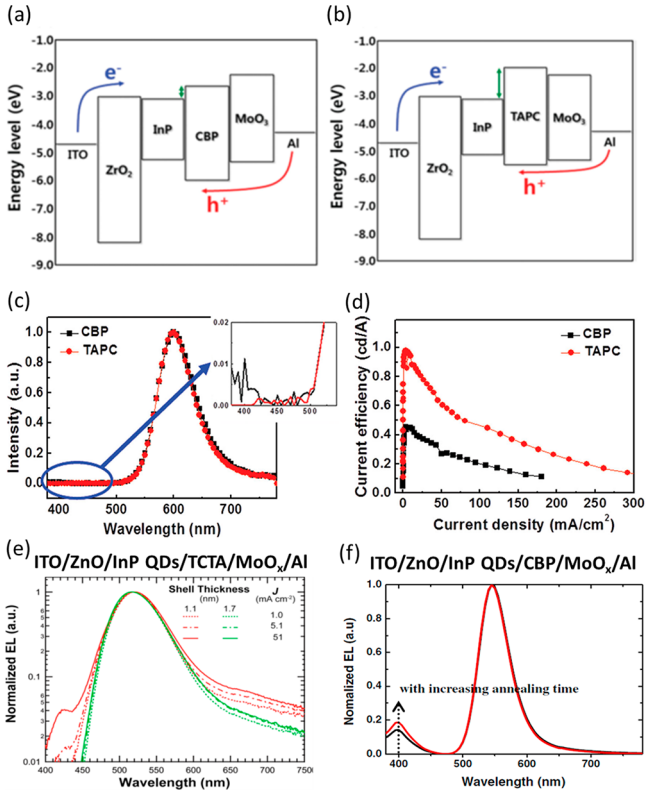

Figure 6. (a and b) Device structures, (c) EL emission spectra, and (d) current efficiencies of the inverted InP-based QLEDs using CBP or TAPC as HTL. Reprinted with permission from ref 86. Copyright 2016 John Wiley and Sons. The inset in panel c shows parasitic emission in the device using CBP as HTL. (e) EL emission spectra of the inverted InP-based QLED using TCTA as HTL. Reprint from ref 78. Copyright 2013 American Chemical Society. (f) EL emission spectra of the inverted InP-based QLED using CBP as HTL. Reprinted with permission from ref 88. Copyright 2015 The Japan Society of Applied Physics.

Most of the reported green InP QDs exhibited parasitic emission. To solve the problem from the anode side, more balanced carrier injection by improving hole injection was tried. It was very effective to improve hole injection by using the organic molecules with deep-lying highest occupied molecular orbitals (HOMOs) and high hole mobility as the HTL.[84,85] However, the above strategies seemed not helpful to suppress the parasitic emission in InP QLEDs. In ref 86, as shown in Figure 6a−d, 4,4′-cyclohexylidenebis[*N*,*N*-bis(4-methylphenyl)benzenamine] (TAPC) or CBP was used as HTL in inverted InP QLED with the structure ITO/ZrO_2/InP QDs/TAPC or CBP/MoO_3/Al. The energy levels of TAPC were the same as those of TCTA. However, the energy levels of the CBP were deeper. The hole mobility of TAPC and CBP were both in the order of 10^{-3}−10^{-2} $cm^2 V^{-1} s^{-1}$. Because of the deep-lying HOMO and high hole mobility, CBP was usually used to reduce hole injection barrier and improve the performance in CdSe-based QLEDs.[84,87] However, it was very surprising that using CBP as the HTL in InP QLEDs performed worse with slight parasitic emission and lower EQE, compared to the InP QLED using TAPC. The above results were also consistent with the results reported in refs 78 and88, as shown in Figure 6e,f. In ref 78, the structure ITO/ZnO/InP QDs/TCTA/MoO_x/Al was used for green InP QLED. Only very weak parasitic emission from TCTA was observed in the QLEDs using InP QDs with very thin shells. On the other hand, the structure ITO/ZnO/InP QDs/CBP/MoO_x/Al used in ref 88 showed significant parasitic emission, i.e., 20% of the peak intensity of the EL emission. Therefore, we believe that reducing hole injection barrier is not the solution for the problem of parasitic emission in InP-based QLEDs.

Figure 7a−c also shows our unpublished results. PTAA, with both higher lowest unoccupied molecular orbital (LUMO) and HOMO, was used to replace TFB in InP-based QLED. With PTAA, the EQE in both very low and very high current regions was higher, and the parasitic emission from HTL was completely gone. It should be noted that the hole injection barrier becomes higher in devices using PTAA as the HTL. On the other hand, the very high LUMO in PTAA placed a strong barrier to prevent the electrons from transferring into PTAA. In ref 79, the structures ITO/PEDOT:PSS/TFB or PVK/InP QDs/ZnO/Al were used to compare the effects between TFB and PVK. The InP QDs in this work emitted red light because of the large particle size, which suffered less from parasitic emission. However, as shown in Figure 7d−f, the device using TFB as the HTL still showed observable parasitic emission, while the device using PVK as HTL completely suppressed the parasitic emission. The LUMO level of PVK is 0.4 eV higher than that of TFB. The LUMO level of TFB was not high enough to block the electron transfer from InP QDs to the TFB layer. Therefore, we concluded that (a) unlike the device structure in CdSe-based QLEDs, an HTL with a very deep-lying HOMO was not necessary in InP QLEDs and (b) the high LUMO level in the HTL was important for suppressing parasitic emission.

https://dx.doi.org/10.1021/acsenergylett.9b02824
ACS Energy Lett. 2020, 5, 1095−1106

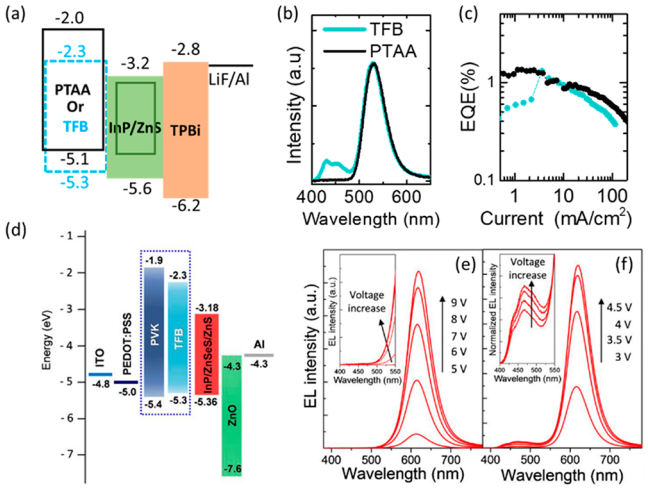

Figure 7. (a) Device structure, (b) EL emission spectra, and (c) EQE of conventional InP-based QLED using TFB or PTAA as HTL. (d) The device structure of InP-based QLED using PVK or TFB as HTL. The EL emission spectra of devices using (e) PVK (f) TFB as HTL. Panels d–f are reprinted with permission from ref 79. Copyright 2016 The Optical Society.

We concluded that (a) unlike the device structure in CdSe-based QLEDs, an HTL with a very deep-lying HOMO was not necessary in InP QLEDs and (b) the high LUMO level in the HTL was important for suppressing parasitic emission.

Because of the high-lying CBM of InP QDs, reduction of electron injection barrier was thought to be the correct direction for optimizing the ETL in InP QLEDs. However, after thorough analysis of the published results from the literature and our own unpublished results, we realized that this was not always correct, especially in InP-based QLEDs with poor electron confinement. From 2013 to 2017, there were four publications with careful studies on the ETL in InP QLEDs.[78,88−90] The following paragraphs summarize the analysis on the results from these four publications.

In ref 78, a thin layer of poly-[(9,9-bis(30-(*N*,*N*-dimethylamino)propyl)-2,7-fluorene)-*alt*-2,7-(9,9-ioctylfluorene)] (PFN) was inserted between ZnO and InP QDs in the structure ITO/ZnO/PFN/InP QDs/TCTA/MoO_3/Al, as shown in Figure 8a. Ref 78 claimed that PFN reduced the electron injection barrier and achieved more balanced carrier injection, so the InP QLEDs with PFN were better. PFN is a kind of conjugated polyelectrolyte, which had been widely used in organic optoelectronic devices such as organic solar cells (OPVs) and organic light-emitting diodes.[91−94] PFN usually induced an interfacial dipole and shifted the Fermi levels of the active layers upward (carrier generation layer in OPV or emissive layer in LED); that is, the energy levels of the active layers shifted downward at the active layer/cathode interface, as illustrated in Figure 8a,b. However, there was no convincing data to conclude that the improved EQE was due to the reduced electron injection barrier. No evidence showed that PFN improved the current in the electron-only device. Another experimental fact contradictory to the conclusion was that the luminance of InP QLEDs with PFN continuously decreased as the concentration of PFN increased from 0 to 1.5 mg/mL. This fact seemed to imply PFN induced less efficient electron injection. It is known that PFN is a conjugated polymer with decent carrier mobility, so the optimal thickness and solution concentration of PFN used in organic LEDs with the above similar structure were usually 10−15 nm and 1.5−2.5 mg/mL, respectively.[95,96] However, in ref 78, InP QLEDs using 0.5 mg/mL PFN performed the best, and it continuously deteriorated as the concentration increased. There was no data between 0 and the best concentration of 0.5 mg/mL. The improvement remained mysterious. As one more reference, another recent publication claimed that PFN improved the performance of CdSe QLEDs because of improved hole injection, rather than electron injection.[97]

Later in 2015, the experimental facts from two similar publications seemed to suggest less efficient electron injection, rather than improved electron injection, was helpful to improve the performance of green InP QLEDs.[88,89] It has also been reported many times that suppression of electron injection improved the performance of CdSe-based QLEDs by inserting insulating organic polymers or electron-blocking polymers between QDs and ZnO layer.[23,98,99] This was explained by the prevention of excess electron injection and better balance of carriers. The two references[88,89] studied how the preparation conditions of ZnO interlayer affect the performance of InP QLED with the same device structure. The device structure with energy levels is shown in Figure 9a. As shown in Figure 9b, lower efficiency and more serious parasitic emission were observed if ZnO sol−gel was annealed at higher temperatures. It claimed that 150 °C annealing was the best. However, another article[89] from the same group

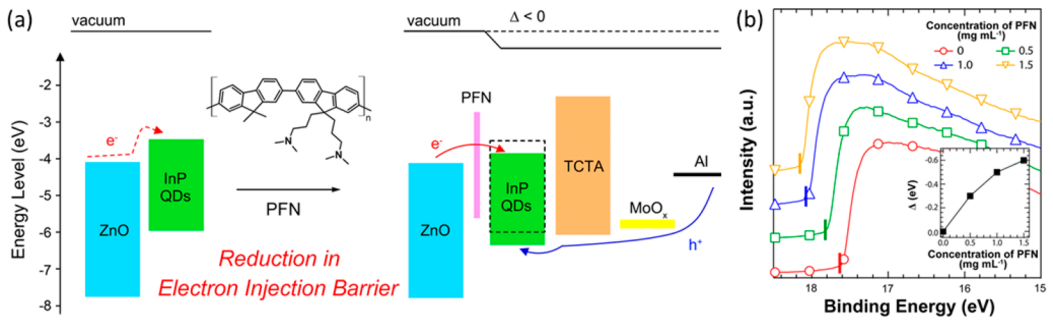

Figure 8. (a) Device structures of the InP-based QLED showing that the Fermi level and vacuum level of the layers on top of the PFN were shifted downward. (b) Relationship between the concentration of the PFN and the energy shift of the Fermi level. Reprinted from ref 78. Copyright 2013 American Chemical Society.

https://dx.doi.org/10.1021/acsenergylett.9b02824
ACS Energy Lett. 2020, 5, 1095−1106

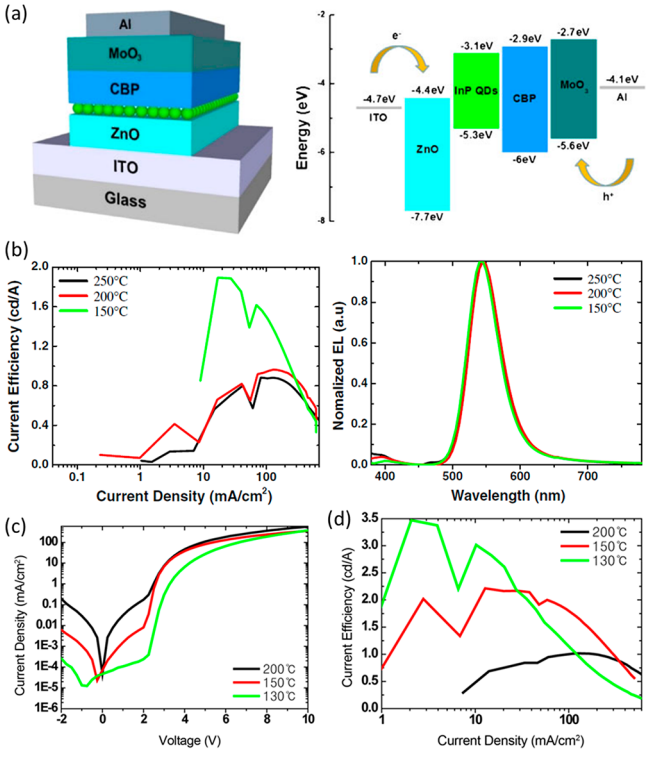

Figure 9. (a) Device structure with energy level alignments. (b) Impacts of the annealing temperature of ZnO on the current efficiency and parasitic emission in the devices. Panels a and b are reprinted with permission from ref 88. Copyright 2015 The Japan Society of Applied Physics. (c) Current−Voltage characteristics and (d) current efficiencies of the InP QLEDs with ZnO layer annealed at different temperatures. Reprinted with permission from ref 89. Copyright 2015 Springer Nature.

showed that 130 °C annealed ZnO sol−gel was even better, as shown in Figure 9c. Data from both of the articles showed the efficiency was improved with lower current and worse electron injection, as shown in Figure 9c,d. It is known that the crystallization and electron conductivity of ZnO sol−gel film were better under higher annealing temperature. All the experimental facts in refs 88 and 89 suggested that the electron injection should be suppressed with less conductive ZnO to improve the efficiency of InP QLEDs. However, it was a pity to claim that the improvement of InP QLEDs with ethanolamine-treated ZnO was due to more efficient electron injection in ref 89.

In 2017, Wang reported that replacing ZnO by ZnMgO as ETL improved the performance of InP QLEDs.[90] The device structures with energy level alignments were shown in Figure 10a. The reason for the improvement was attributed to the higher CBM of ZnMgO and improved electron injection. However, current−voltage characteristics of the devices shown in Figure 10b suggested the contrary result; that is, replacing ZnO by ZnMgO suppressed the electron injection and reduced the current. In our opinion, the improved performance of the InP QLED using ZnMgO was due to the fewer gap states in ZnMgO. Similar explanations were made for the improvements of organic photovoltaics (OPV) using ZnO as electron extraction layer.[100−102] Previous works showed that the trap states in ZnO were passivated by UV exposure or Al doping, resulting in better performance of OPV.[103,104] In ref 104, when Al was slightly doped into ZnO nanoparticles, the absorption

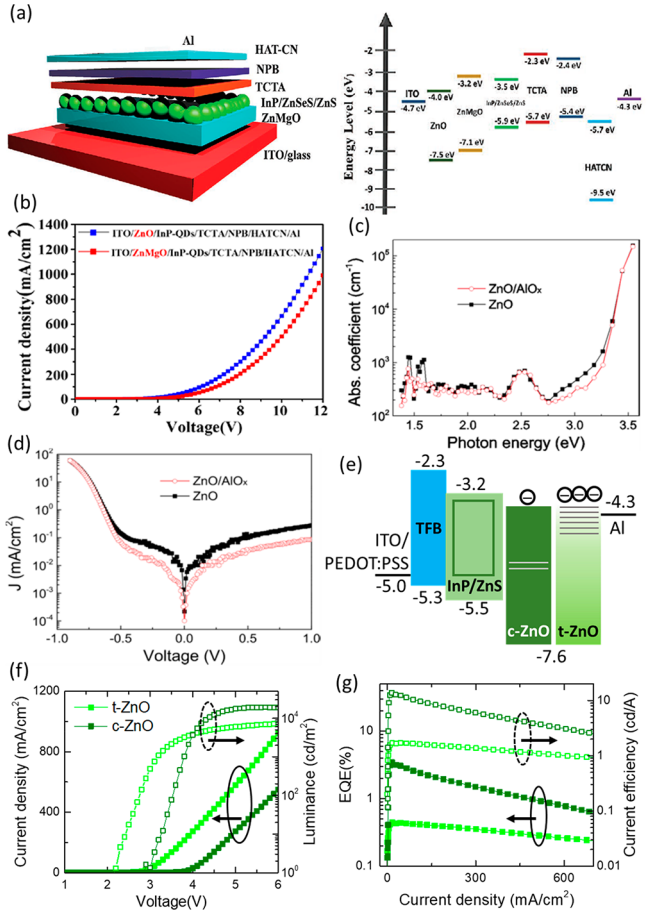

Figure 10. (a) Device structure and energy level alignments and (b) current−voltage characteristics of the InP/ZnSeS/ZnS QLED studied in ref 90. Panels a and b are reprinted with permission from ref 90. Copyright 2017 John Wiley and Sons. (c) Absorption by the gap states in ZnO and Al:ZnO. (d) Dark current−voltage characteristics of the photodiodes using ZnO and Al:ZnO as cathode interlayers. Panels c and d are reprinted from ref 104. Copyright 2016 American Chemical Society. (e) Device structure, (f) current−voltage−luminance characteristics, and (g) EQE and CE.

by the subgap states (<3.3 eV) of ZnO decreased significantly, as shown in Figure 10c. The leakage current in the OPV device with ZnO:Al as electron extraction layer was reduced, leading to improved device performance (Figure 10d). The improvement of InP QLEDs using ZnMgO ETL may be explained in similar ways; that is, doping of Mg passivated the subgap states. Previous studies on ZnO showed that Mg doping increased the band gap and reduced the electron concentration in ZnO.[105,106] At room temperature, the high intrinsic carrier concentration in oxide semiconductors usually originates from the thermal excitation from gap states.[107] Reduced electron concentration and conductivity in oxide semiconductors at room temperature implied fewer gap states.

To confirm it was the passivation of gap states and reduced electron conductivity that were responsible for the improvement of InP QLEDs using ZnMgO as ETL, two InP QLEDs using two different kinds of ZnO nanoparticles, i.e., c-ZnO and t-ZnO, were fabricated. c-ZnO showed poor conductivity, while t-ZnO showed two orders higher conductivity. As explained in the previous paragraph, this was due to a higher density of gap states near the CBM in t-ZnO than in c-ZnO.

https://dx.doi.org/10.1021/acsenergylett.9b02824
ACS Energy Lett. 2020, 5, 1095−1106

Therefore, c-ZnO actually refers to crystalline-ZnO, and t-ZnO refers to trap states-ZnO. Both c-ZnO and t-ZnO were synthesized according to the general guidelines in the patent in ref 108. c-ZnO was synthesized in the methanol with very slow reaction (>3 h), while t-ZnO was synthesized in the mixture of dimethyl sulfoxide (DMSO) and ethanol with fast reaction rate. As shown in Figure 10e,f, the InP QLEDs using t-ZnO showed higher current, implying higher electron concentration and conductivity in t-ZnO, in comparison to InP QLEDs using c-ZnO. The InP QLEDs using c-ZnO showed higher EQE (3.5%), but also higher turn-on voltage. In the QLEDs with c-ZnO as ETL, the luminance was lower under small bias but surpassed that of the device using t-ZnO when the bias was over 4 V. Under small bias, the electrons injected into the QLED using c-ZnO as ETL was not enough to achieve high luminance. On the contrary, the electron injection in the QLED using t-ZnO was too efficient because of too many gap states and the high carrier concentration in t-ZnO. As a result, the parasitic emission was observed in InP QLEDs using t-ZnO. On the other hand, exciton quenching at the QD and ZnO interface was less likely in the QLED using c-ZnO because of fewer traps near the CBM, resulting in a higher EQE and current efficiency, as shown in Figure 10g. Therefore, the gap states and electron conductivity of ZnO or doped ZnO were more important concerns, compared to the CBM alignments with InP QDs. The above arguments are also consistent with the conclusions in Chen, Tang, and co-worker's work published recently.[109] This work studied the effects of differently modified ZnO in InP QLEDs and concluded that the combination of chloride-passivation of surface trap states and Mg doping of ZnO NPs can prevent exciton quenching at the QDs/ETL interface.

Since the first report of InP-based QLED in 2011, the performance of InP-based QLED was greatly enhanced through the efforts on the synthesis of high-quality InP QDs and optimization of the QLED device structure. There remained many challenges for achieving high-performance InP-based QLEDs. High PLQY of InP QDs in solution did not guarantee high performance of InP-based QLEDs. The device physics was not well-studied or understood in the recent decade. Unlike the problem of poor hole injection in CdSe-based QLEDs, the key concern in InP-based QLEDs was the too-active electrons in the device. To address this problem, possible solutions were summarized from the following three perspectives.

From the above analysis, there are road maps to boost the performance of InP QLEDs from the following aspects. The following is summary of the guidelines for synthesizing InP/shell/shell structures for high-performance InP QLEDs: (a) High-quality crystallization of InP core without oxidation or structural defects was required. (b) A thick shell with good passivation of interface traps was required to confine the carriers and prevent electron trapping. (c) The interfaces between each portion in the structure of core/shell/shell should be sharply defined so that the interpenetrations between the chemical compositions in the core and shells can be prevented. The above three strategies are more difficult to be applied in green InP QDs because of the extremely small particle size, in comparison to red InP QDs. These might be the main reasons for the superior performance of red InP QLEDs over green InP QLEDs. The following is a summary of the guidelines for choosing the HTL in InP QLEDs: (a) A very high-lying LUMO of the HTL is very important to block the electron leakage at the HTL/QDs interface and suppress the parasitic emission. (b) High hole mobility is required to adjust the location of exciton formation. The electron confinement in InP QLEDs was so poor that the electrons are easily transported to the interface of HTL/QDs. Faster hole transport is expected to shift the location of exciton formation to the middle of the QD layer, so that the possible exciton quenching at the HTL/QD interface could be avoided. (c) An HTL with a HOMO level deeper than −5.3 eV is not necessary in InP QLEDs. A summary of the guidelines for choosing the ETL in InP QLEDs is as follows: (a) Electron injection was always too efficient in InP QLEDs with ZnO or doped ZnO as ETL, though the CBM of InP QDs was usually very high. (b) The electron mobility and conductivity of oxide semiconductor ETL should be suppressed to reduce the energetic activity of electrons in InP QLEDs. (c) The passivation of gap states and reduced electron concentration in oxide semiconductor ETL were more important in InP QLEDs, in comparison to the CBM alignments.

Electron injection was always too efficient in InP QLEDs with ZnO or doped ZnO as the ETL, though the CBM of InP QDs was usually very high.

As the synthetic process is improved to synthesize better InP QDs with different electronic properties in the future, the specific approaches for device optimization introduced in this work or previous publications may no longer apply. However, the ultimate principle is to ensure both efficient exciton formation inside the InP core and efficient carrier (both hole and electron) injection across the InP QD surface. In some previous works, the conclusions regarding device physics in InP QLEDs usually contradicted with their own experimental data. This reminds us that discussions about device physics should be based on thorough and comprehensive analysis of the experimental data, including current−luminance−voltage characteristics, characteristics of emission spectra, spectroscopy studies, direct surface characterizations, etc.

AUTHOR INFORMATION

Corresponding Author

Xiao Wei Sun − *Guangdong University Key Lab for Advanced Quantum Dot Displays and Lighting, Shenzhen Key Laboratory for Advanced Quantum Dot Displays and Lighting, and Department of Electrical and Electronic Engineering, Southern University of Science and Technology, Shenzhen 518055, China; Shenzhen Planck Innovation Technologies Pte Ltd, Shenzhen, China;* orcid.org/0000-0002-2840-1880; Email: sunxw@sustech.edu.cn

Authors

Zhenghui Wu − *Guangdong University Key Lab for Advanced Quantum Dot Displays and Lighting, Shenzhen Key Laboratory for Advanced Quantum Dot Displays and Lighting, and Department of Electrical and Electronic Engineering, Southern University of Science and Technology, Shenzhen 518055, China*

Pai Liu − *Guangdong University Key Lab for Advanced Quantum Dot Displays and Lighting, Shenzhen Key Laboratory for Advanced Quantum Dot Displays and Lighting, and Department of Electrical and Electronic Engineering, Southern University of Science and Technology, Shenzhen 518055, China*

https://dx.doi.org/10.1021/acsenergylett.9b02824
ACS Energy Lett. 2020, 5, 1095−1106

Wenda Zhang − *Guangdong University Key Lab for Advanced Quantum Dot Displays and Lighting, Shenzhen Key Laboratory for Advanced Quantum Dot Displays and Lighting, and Department of Electrical and Electronic Engineering, Southern University of Science and Technology, Shenzhen 518055, China*

Kai Wang − *Guangdong University Key Lab for Advanced Quantum Dot Displays and Lighting, Shenzhen Key Laboratory for Advanced Quantum Dot Displays and Lighting, and Department of Electrical and Electronic Engineering, Southern University of Science and Technology, Shenzhen 518055, China; Shenzhen Planck Innovation Technologies Pte Ltd, Shenzhen, China*

Complete contact information is available at: https://pubs.acs.org/10.1021/acsenergylett.9b02824

Notes

The authors declare no competing financial interest.

Biographies

Zhenghui Wu is working as a research assistant professor at Southern University of Science and Technology, China. He received his both B.Sc. (2011) and Ph.D. (2015) in physics from Hong Kong Baptist University. He worked as a postdoctoral researcher at University of California San Diego from 2016 to 2019.

Pai Liu is working as a research assistant professor at Southern University of Science and Technology, China. She received her M.Sc. in materials science and engineering from Arizona State University and her Ph.D. in chemistry from University of Limerick. Her research interests include semiconductor nanocrystals and quantum dots.

Wenda Zhang is currently pursuing his Ph.D. degree at General Research Institute, China. He is also a visiting Ph.D. candidate at Southern University of Science and Technology. His received his undergraduate degree in rare earth engineering from Jiangxi University of Science and Technology.

Kai Wang is an associate professor at Southern University of Science and Technology. He received his Ph.D. (2011) in optical engineering at Huazhong University of Science and Technology and Wuhan National Laboratory for Optoelectronics and B.Sc. (2006) in optical information science and technology at Huazhong University of Science and Technology.

Xiao Wei Sun is the Chair professor of EEE at Southern University of Science and Technology. He received his B.Eng. in photonics (1990) and M.Eng. in optical instrumentation (1992) from Tianjin University, China. He received Ph.D. degree from the Hong Kong University of Science and Technology. Web page: https://eee.sustc.edu.cn/?academic_category=disciplinary&lang=en

■ ACKNOWLEDGMENTS

We acknowledge support from the Ministry of Science and Technology of China (Nos. 2016YFB0401702 and 2017YFE0120400), National Natural Science Foundation of China (Nos. 61674074, 61875082, and 61405089), Guangdong Province's Key R&D Program: Micro-LED Display and Ultrahigh Brightness Microdisplay Technology (Project No. 2019B010925001), Environmentally Friendly Quantum Dots Luminescent Materials (Project No. 2019B010924001), Guangdong University Key Laboratory for Advanced Quantum Dot Displays and Lighting (No.2017KSYS007), Distinguished Young Scholar of Natural Science Foundation of Guangdong (No. 2017B030306010), Shenzhen Key Laboratory for Advanced Quantum Dot Displays and Lighting (No. ZDSYS201707281632549), Shenzhen Peacock Team Project (No. KQTD2016030111203005), and Shenzhen Innovation Project (No. JSGG20170823160757004).

■ REFERENCES

(1) Fang, M. H.; Leano, J. L.; Liu, R. S. Control of Narrow-Band Emission in Phosphor Materials for Application in Light-Emitting Diodes. *ACS Energy Lett.* **2018**, *3*, 2573−2586.
(2) Park, J. H.; Kim, D. Y.; Schubert, E. F.; Cho, J.; Kim, J. K. Fundamental Limitations of Wide-Bandgap Semiconductors for Light-Emitting Diodes. *ACS Energy Lett.* **2018**, *3*, 655−662.
(3) Lin, H.; Zhou, C.; Tian, Y.; Siegrist, T.; Ma, B. Low-Dimensional Organometal Halide Perovskites. *ACS Energy Lett.* **2018**, *3*, 54−62.
(4) Park, M. H.; Kim, J. S.; Heo, J. M.; Ahn, S.; Jeong, S. H.; Lee, T. W. Boosting Efficiency in Polycrystalline Metal Halide Perovskite Light-Emitting Diodes. *ACS Energy Lett.* **2019**, *4*, 1134−1149.
(5) Brus, L. Electronic Wave Functions in Semiconductor Clusters: Experiment and Theory. *J. Phys. Chem.* **1986**, *90*, 2555−2560.
(6) Alivisatos, A. P. Semiconductor Clusters, Nanocrystals,and Quantum Dots. *Science (Washington, DC, U. S.)* **1996**, *271*, 933.
(7) Kagan, C. R.; Lifshitz, E.; Sargent, E. H.; Talapin, D. V. Building Devices from Colloidal Quantum Dots. *Science (Washington, DC, U. S.)* **2016**, *353*, aac5523.
(8) Peng, X.; Schlamp, M. C.; Kadavanich, A. V.; Alivisatos, A. P. Epitaxial Growth of Highly Luminescent CdSe/CdS Core/Shell Nanocrystals with Photostability and Electronic Accessibility. *J. Am. Chem. Soc.* **1997**, *119*, 7019−7029.
(9) Hines, M. A.; Guyot-Sionnest, P. Synthesis and Characterization of Strongly Luminescing ZnS-Capped CdSe Nanocrystals. *J. Phys. Chem.* **1996**, *100*, 468−471.
(10) Li, J. J.; Wang, Y. A.; Guo, W.; Keay, J. C.; Mishima, T. D.; Johnson, M. B.; Peng, X. Large-Scale Synthesis of Nearly Monodisperse CdSe/CdS Core/Shell Nanocrystals Using Air-Stable Reagents via Successive Ion Layer Adsorption and Reaction. *J. Am. Chem. Soc.* **2003**, *125*, 12567−12575.
(11) Dai, X.; Deng, Y.; Peng, X.; Jin, Y. Quantum-Dot Light-Emitting Diodes for Large-Area Displays: Towards the Dawn of Commercialization. *Adv. Mater.* **2017**, *29*, 1607022.
(12) Jang, E.; Jun, S.; Jang, H.; Lim, J.; Kim, B.; Kim, Y. White-Light-Emitting Diodes with Quantum Dot Color Converters for Display Backlights. *Adv. Mater.* **2010**, *22*, 3076−3080.
(13) Zhu, R.; Luo, Z.; Chen, H.; Dong, Y.; Wu, S.-T. Realizing Rec 2020 Color Gamut with Quantum Dot Displays. *Opt. Express* **2015**, *23*, 23680.
(14) Chen, H.; He, J.; Wu, S. Recent Advances on Quantum-Dot-Enhanced Liquid-Crystal Displays. *IEEE J. Sel. Top. Quantum Electron.* **2017**, *23*, 1900611.
(15) Chen, H. W.; Zhu, R. D.; He, J.; Duan, W.; Hu, W.; Lu, Y. Q.; Li, M. C.; Lee, S. L.; Dong, Y. J.; Wu, S. T. Going beyond the Limit of an LCD's Color Gamut. *Light: Sci. Appl.* **2017**, *6*, e17043−10.
(16) Talapin, D. V.; Rogach, A. L.; Kornowski, A.; Haase, M.; Weller, H. Highly Luminescent Monodisperse CdSe and CdSe/ZnS Nanocrystals Synthesized in a Hexadecylamine-Trioctylphosphine Oxide-Trioctylphospine Mixture. *Nano Lett.* **2001**, *1*, 207−211.
(17) Kudera, S.; Zanella, M.; Giannini, C.; Rizzo, A.; Li, Y.; Gigli, G.; Cingolani, R.; Ciccarella, G.; Spahl, W.; Parak, W. J.; et al. Sequential Growth of Magic-Size CdSe Nanocrystals. *Adv. Mater.* **2007**, *19*, 548−552.
(18) Danek, M.; Jensen, K. F.; Murray, C. B.; Bawendi, M. G. Synthesis of Luminescent Thin-Film CdSe/ZnSe Quantum Dot Composites Using CdSe Quantum Dots Passivated with an Overlayer of ZnSe. *Chem. Mater.* **1996**, *8*, 173−180.
(19) Reiss, P.; Bleuse, J.; Pron, A. Highly Luminescent CdSe/ZnSe Core/Shell Nanocrystals of Low Size Dispersion. *Nano Lett.* **2002**, *2*, 781−784.
(20) Talapin, D. V.; Mekis, I.; Götzinger, S.; Kornowski, A.; Benson, O.; Weller, H. CdSe/CdS/ZnS and CdSe/ZnSe/ZnS Core-Shell-Shell Nanocrystals. *J. Phys. Chem. B* **2004**, *108*, 18826−18831.

(21) Lim, J.; Jun, S.; Jang, E.; Baik, H.; Kim, H.; Cho, J. Preparation of Highly Luminescent Nanocrystals and Their Application to Light-Emitting Diodes. *Adv. Mater.* **2007**, *19*, 1927−1932.
(22) Wang, X.; Li, W.; Sun, K. Stable Efficient CdSe/CdS/ZnS Core/Multi-Shell Nanophosphors Fabricated through a Phosphine-Free Route for White Light-Emitting-Diodes with High Color Rendering Properties. *J. Mater. Chem.* **2011**, *21*, 8558−8565.
(23) Dai, X.; Zhang, Z.; Jin, Y.; Niu, Y.; Cao, H.; Liang, X.; Chen, L.; Wang, J.; Peng, X. Solution-Processed, High-Performance Light-Emitting Diodes Based on Quantum Dots. *Nature* **2014**, *515*, 96−99.
(24) Zhang, H.; Sun, X.; Chen, S. Over 100 Cd A−1 Efficient Quantum Dot Light-Emitting Diodes with Inverted Tandem Structure. *Adv. Funct. Mater.* **2017**, *27*, 1−8.
(25) Zhang, H.; Chen, S.; Sun, X. W. Efficient Red/Green/Blue Tandem Quantum-Dot Light-Emitting Diodes with External Quantum Efficiency Exceeding 21%. *ACS Nano* **2018**, *12*, 697−704.
(26) Wang, L.; Lin, J.; Hu, Y.; Guo, X.; Lv, Y.; Tang, Z.; Zhao, J.; Fan, Y.; Zhang, N.; Wang, Y.; et al. Blue Quantum Dot Light-Emitting Diodes with High Electroluminescent Efficiency. *ACS Appl. Mater. Interfaces* **2017**, *9*, 38755−38760.
(27) Kolonel, L. N. With Renal Cancer. *Cancer* **1976**, *37*, 1782−1787.
(28) Järup, L. Hazards of Heavy Metal Contamination. *Br. Med. Bull.* **2003**, *68*, 167−182.
(29) Chen, F.; Guan, Z.; Tang, A. Nanostructure and Device Architecture Engineering for High-Performance Quantum-Dot Light-Emitting Diodes. *J. Mater. Chem. C* **2018**, *6*, 10958−10981.
(30) Guzelian, A. A.; Katari, J. E. B.; Kadavanich, A. V.; Banin, U.; Hamad, K.; Juban, E.; Alivisatos, A. P.; Wolters, R. H.; Arnold, C. C.; Heath, J. R. Synthesis of Size-Selected, Surface-Passivated InP Nanocrystals. *J. Phys. Chem.* **1996**, *100*, 7212−7219.
(31) Mićić, O. I.; Cheong, H. M.; Fu, H.; Zunger, A.; Sprague, J. R.; Mascarenhas, A.; Nozik, A. J. Size-Dependent Spectroscopy of InP Quantum Dots. *J. Phys. Chem. B* **1997**, *101*, 4904−4912.
(32) Wang, A.; Shen, H.; Zang, S.; Lin, Q.; Wang, H.; Qian, L.; Niu, J.; Li, L. S. Bright, Efficient, and Color-Stable Violet ZnSe-Based Quantum Dot Light-Emitting Diodes. *Nanoscale* **2015**, *7*, 2951−2959.
(33) Xiang, C.; Koo, W.; Chen, S.; So, F.; Liu, X.; Kong, X.; Wang, Y. Solution Processed Multilayer Cadmium- Free Blue/Violet Emitting Quantum Dots Light Emitting Diodes. *Appl. Phys. Lett.* **2012**, *101*, 053303.
(34) Huang, X.; Yu, R.; Yang, X.; Xu, X.; Zhang, H.; Zhang, D. Efficient CuInS2/ZnS Based Quantum Dot Light Emitting Diodes by Engineering the Exciton Formation Interface. *J. Lumin.* **2018**, *202*, 339−344.
(35) Li, L.; Pandey, A.; Werder, D. J.; Khanal, B. P.; Pietryga, J. M.; Klimov, V. I. Efficient Synthesis of Highly Luminescent Copper Indium Sulfide-Based Core/Shell Nanocrystals with Surprisingly Long-Lived Emission. *J. Am. Chem. Soc.* **2011**, *133*, 1176−1179.
(36) Wang, F.; Chen, Y. H.; Liu, C. Y.; Ma, D. G. White Light-Emitting Devices Based on Carbon Dots' Electroluminescence. *Chem. Commun.* **2011**, *47*, 3502−3504.
(37) Kim, B. H.; Cho, C. H.; Mun, J. S.; Kwon, M. K.; Park, T. Y.; Kim, J. S.; Byeon, C. C.; Lee, J.; Park, S. J. Enhancement of the External Quantum Efficiency of a Silicon Quantum Dot Light-Emitting Diode by Localized Surface Plasmons. *Adv. Mater.* **2008**, *20*, 3100−3104.
(38) Shen, H.; Wang, H.; Li, X.; Niu, J. Z.; Wang, H.; Chen, X.; Li, L. S. Phosphine-Free Synthesis of High Quality ZnSe, ZnSe/ZnS, and Cu-, Mn-Doped ZnSe Nanocrystals. *Dalt. Trans.* **2009**, No. 47, 10534−10540.
(39) Ji, W.; Jing, P.; Xu, W.; Yuan, X.; Wang, Y.; Zhao, J.; Jen, A. K. Y. High Color Purity ZnSe/ZnS Core/Shell Quantum Dot Based Blue Light Emitting Diodes with an Inverted Device Structure. *Appl. Phys. Lett.* **2013**, *103*, 053106.
(40) Kim, J. H.; Yang, H. High-Efficiency Cu-In-S Quantum-Dot-Light-Emitting Device Exceeding 7%. *Chem. Mater.* **2016**, *28*, 6329−6335.
(41) Cheng, K. Y.; Anthony, R.; Kortshagen, U. R.; Holmes, R. J. High-Efficiency Silicon Nanocrystal Light-Emitting Devices. *Nano Lett.* **2011**, *11*, 1952−1956.
(42) Kim, D. H.; Kim, T. W. Ultrahigh Current Efficiency of Light-Emitting Devices Based on Octadecylamine-Graphene Quantum Dots. *Nano Energy* **2017**, *32*, 441−447.
(43) Battaglia, D.; Peng, X. Formation of High Quality InP and InAs Nanocrystals in a Noncoordinating Solvent. *Nano Lett.* **2002**, *2*, 1027−1030.
(44) Li, L.; Reiss, P. One-Pot Synthesis of Highly Luminescent InP/ZnS Nanocrystals without Precursor Injection. *J. Am. Chem. Soc.* **2008**, *130*, 11588−11589.
(45) Zhang, H.; Hu, N.; Zeng, Z.; Lin, Q.; Zhang, F.; Tang, A.; Jia, Y.; Li, L. S.; Shen, H.; Teng, F.; et al. High-Efficiency Green InP Quantum Dot-Based Electroluminescent Device Comprising Thick-Shell Quantum Dots. *Adv. Opt. Mater.* **2019**, *7*, 1801602.
(46) Won, Y.; Cho, O.; Kim, T.; Chung, D.; Kim, T.; Chung, H.; Jang, H.; Lee, J.; Kim, D.; Jang, E. Highly Efficient and Stable InP/ZnSe/ZnS Quantum Dot Light-Emitting Diodes. *Nature* **2019**, *575*, 634.
(47) Lim, J.; Bae, W. K.; Lee, D.; Nam, M. K.; Jung, J.; Lee, C.; Char, K.; Lee, S. Inp@znses, Core@composition Gradient Shell Quantum Dots with Enhanced Stability. *Chem. Mater.* **2011**, *23*, 4459−4463.
(48) Li, Y.; Hou, X.; Dai, X.; Yao, Z.; Lv, L.; Jin, Y.; Peng, X. Stoichiometry-Controlled InP-Based Quantum Dots: Synthesis, Photoluminescence, and Electroluminescence. *J. Am. Chem. Soc.* **2019**, *141*, 6448−6452.
(49) Colvin, V. L.; Schlamp, M. C.; Alivisatos, A. P. Light-Emitting Diodes Made from Cadmium Selenide Nanocrystals and a Semiconducting Polymer. *Nature* **1994**, *370*, 354−357.
(50) Coe, S.; Woo, W. K.; Bawendi, M.; Bulović, V. Electroluminescence from Single Monolayers of Nanocrystals in Molecular Organic Devices. *Nature* **2002**, *420*, 800−803.
(51) Caruge, J. M.; Halpert, J. E.; Bulović, V.; Bawendi, M. G. NiO as an Inorganic Hole-Transporting Layer in Quantum-Dot Light-Emitting Devices. *Nano Lett.* **2006**, *6*, 2991−2994.
(52) Shirasaki, Y.; Supran, G. J.; Bawendi, M. G.; Bulović, V. Emergence of Colloidal Quantum-Dot Light-Emitting Technologies. *Nat. Photonics* **2013**, *7*, 13−23.
(53) Bozyigit, D.; Wood, V. Challenges and Solutions for High-Efficiency Quantum Dot-Based LEDs. *MRS Bull.* **2013**, *38*, 731−736.
(54) Pietryga, J. M.; Park, Y. S.; Lim, J.; Fidler, A. F.; Bae, W. K.; Brovelli, S.; Klimov, V. I. Spectroscopic and Device Aspects of Nanocrystal Quantum Dots. *Chem. Rev.* **2016**, *116*, 10513−10622.
(55) Micic, O. I.; Sprague, J. R.; Curtis, C. J.; Jones, K. M.; Machol, J. L.; Nozik, A. J.; Giessen, H.; Fluegel, B.; Mohs, G.; Peyghambarian, N. Synthesis and Characterization of InP, GaP, and GaInP2 Quantum Dots. *J. Phys. Chem.* **1995**, *99*, 7754−7759.
(56) Mićić, O. I.; Ahrenkiel, S. P.; Nozik, A. J. Synthesis of Extremely Small InP Quantum Dots and Electronic Coupling in Their Disordered Solid Films. *Appl. Phys. Lett.* **2001**, *78*, 4022−4024.
(57) Talapin, D. V.; Rogach, A. L.; Mekis, I.; Haubold, S.; Kornowski, A.; Haase, M.; Weller, H. Synthesis and Surface Modification of Amino-Stabilized CdSe, CdTe and InP Nanocrystals. *Colloids Surf., A* **2002**, *202*, 145−154.
(58) Mićić, O. I.; Smith, B. B.; Nozik, A. J. Core-Shell Quantum Dots of Lattice-Matched ZnCdSe2shells on InP Cores: Experiment and Theory. *J. Phys. Chem. B* **2000**, *104*, 12149−12156.
(59) Haubold, S.; Haase, M.; Kornowski, A.; Weller, H. Strongly Luminescent InP/ZnS Core-Shell Nanoparticles. *ChemPhysChem* **2001**, *2*, 331−334.
(60) Xie, R.; Battaglia, D.; Peng, X. Colloidal InP Nanocrystals as Efficient Emitters Covering Blue to Near-Infrared. *J. Am. Chem. Soc.* **2007**, *129*, 15432−15433.
(61) Xu, S.; Ziegler, J.; Nann, T. Rapid Synthesis of Highly Luminescent InP and InP/ZnS Nanocrystals. *J. Mater. Chem.* **2008**, *18*, 2653−2656.

https://dx.doi.org/10.1021/acsenergylett.9b02824
ACS Energy Lett. 2020, 5, 1095−1106

(62) Ryu, E.; Kim, S.; Jang, E.; Jun, S.; Jang, H.; Kim, B.; Kim, S. Step-Wise Synthesis of InP/ZnS Core-Shell Quantum Dots and the Role of Zinc Acetate. *Chem. Mater.* **2009**, *21*, 573.
(63) Lim, K.; Jang, H. S.; Woo, K. Synthesis of Blue Emitting InP/ZnS Quantum Dots through Control of Competition between Etching and Growth. *Nanotechnology* **2012**, *23*, 485609.
(64) Kim, M. R.; Chung, J. H.; Lee, M.; Lee, S.; Jang, D. J. Fabrication, Spectroscopy, and Dynamics of Highly Luminescent Core-Shell InP@ZnSe Quantum Dots. *J. Colloid Interface Sci.* **2010**, *350*, 5−9.
(65) Thuy, U. T. D.; Reiss, P.; Liem, N. Q. Luminescence Properties of In(Zn)P Alloy Core/ZnS Shell Quantum Dots. *Appl. Phys. Lett.* **2010**, *97*, 193104.
(66) Kim, T.; Kim, S. W.; Kang, M.; Kim, S. W. Large-Scale Synthesis of Inpzns Alloy Quantum Dots with Dodecanethiol as a Composition Controller. *J. Phys. Chem. Lett.* **2012**, *3*, 214−218.
(67) Kim, S.; Kim, T.; Kang, M.; Kwak, S. K.; Yoo, T. W.; Park, L. S.; Yang, I.; Hwang, S.; Lee, J. E.; Kim, S. K.; et al. Highly Luminescent InP/GaP/ZnS Nanocrystals and Their Application to White Light-Emitting Diodes. *J. Am. Chem. Soc.* **2012**, *134*, 3804−3809.
(68) Park, J. P.; Lee, J. J.; Kim, S. W. Highly Luminescent InP/GaP/ZnS QDs Emitting in the Entire Color Range via a Heating up Process. *Sci. Rep.* **2016**, *6*, 30094.
(69) Qidwai, A. A.; Woods, J. Defect Levels in Indium and Gallium Doped Zinc Selenide. *J. Cryst. Growth* **1982**, *59*, 217−222.
(70) Moon, Y.; Si, S.; Yoon, E.; Kim, S. J. Low Temperature Photoluminescence Characteristics of Zn-Doped InP Grown by Metalorganic Chemical Vapor Deposition. *J. Appl. Phys.* **1998**, *83*, 2261−2265.
(71) Mocatta, D.; Cohen, G.; Schattner, J.; Millo, O.; Rabani, E.; Banin, U. Heavily Doped Semiconductor Nanocrystal Quantum Dots. *Science (Washington, DC, U. S.)* **2011**, *332*, 77−81.
(72) Bozyigit, D.; Yarema, O.; Wood, V. Origins of Low Quantum Efficiencies in Quantum Dot LEDs. *Adv. Funct. Mater.* **2013**, *23*, 3024−3029.
(73) Shirasaki, Y.; Supran, G. J.; Tisdale, W. A.; Bulović, V. Origin of Efficiency Roll-off in Colloidal Quantum-Dot Light-Emitting Diodes. *Phys. Rev. Lett.* **2013**, *110*, 217403.
(74) Fu, H.; Zunger, A. InP Quantum Dots: Electronic Structure, Surface Effects, and the Redshifted Emission. *Phys. Rev. B: Condens. Matter Mater. Phys.* **1997**, *56*, 1496−1508.
(75) Cao, Y. W.; Banin, U. Growth and Properties of Semiconductor Core/Shell Nanocrystals with InAs Cores. *J. Am. Chem. Soc.* **2000**, *122*, 9692−9702.
(76) Yang, X.; Zhao, D.; Leck, K. S.; Tan, S. T.; Tang, Y. X.; Zhao, J.; Demir, H. V.; Sun, X. W. Full Visible Range Covering InP/ZnS Nanocrystals with High Photometric Performance and Their Application to White Quantum Dot Light-Emitting Diodes. *Adv. Mater.* **2012**, *24*, 4180−4185.
(77) Yang, X.; Divayana, Y.; Zhao, D.; Swee Leck, K.; Lu, F.; Tiam Tan, S.; Putu Abiyasa, A.; Zhao, Y.; Volkan Demir, H.; Wei Sun, X. A Bright Cadmium-Free, Hybrid Organic/Quantum Dot White Light-Emitting Diode. *Appl. Phys. Lett.* **2012**, *101*, 233110.
(78) Lim, J.; Park, M.; Bae, W. K.; Lee, D.; Lee, S.; Lee, C.; Char, K. Highly Efficient Cadmium-Free Quantum Dot Light-Emitting Diodes Enabled by the Direct Formation of Excitons within InP@ZnSeS Quantum Dots. *ACS Nano* **2013**, *7*, 9019−9026.
(79) Jo, J.-H.; Kim, J.-H.; Lee, K.-H.; Han, C.-Y.; Jang, E.-P.; Do, Y. R.; Yang, H. High-Efficiency Red Electroluminescent Device Based on Multishelled InP Quantum Dots. *Opt. Lett.* **2016**, *41*, 3984.
(80) Cao, F.; Wang, S.; Wang, F.; Wu, Q.; Zhao, D.; Yang, X. A Layer-by-Layer Growth Strategy for Large-Size InP/ZnSe/ZnS Core-Shell Quantum Dots Enabling High-Efficiency Light-Emitting Diodes. *Chem. Mater.* **2018**, *30*, 8002−8007.
(81) Kwak, J.; Bae, W. K.; Lee, D.; Park, I.; Lim, J.; Park, M.; Cho, H.; Woo, H.; Yoon, D. Y.; Char, K.; et al. Bright and Efficient Full-Color Colloidal Quantum Dot Light-Emitting Diodes Using an Inverted Device Structure. *Nano Lett.* **2012**, *12*, 2362−2366.
(82) Anthopoulos, T. D.; Markham, J. P. J.; Namdas, E. B.; Samuel, I. D. W.; Lo, S. C.; Burn, P. L. Highly Efficient Single-Layer Dendrimer Light-Emitting Diodes with Balanced Charge Transport. *Appl. Phys. Lett.* **2003**, *82*, 4824−4826.
(83) Sun, Q.; Subramanyam, G.; Dai, L.; Check, M.; Campbell, A.; Naik, R.; Grote, J.; Wang, Y. Highly Efficient Quantum-Dot Light-Emitting Diodes with DNA-CTMA as a Combined Hole-Transporting and Electron-Blocking Layer. *ACS Nano* **2009**, *3*, 737−743.
(84) Ho, M. D.; Kim, D.; Kim, N.; Cho, S. M.; Chae, H. Polymer and Small Molecule Mixture for Organic Hole Transport Layers in Quantum Dot Light-Emitting Diodes. *ACS Appl. Mater. Interfaces* **2013**, *5*, 12369−12374.
(85) Zhang, X.; Dai, H.; Zhao, J.; Wang, S.; Sun, X. All-Solution Processed Composite Hole Transport Layer for Quantum Dot Light Emitting Diode. *Thin Solid Films* **2016**, *603*, 187−192.
(86) Kim, H. Y.; Park, Y. J.; Kim, J.; Han, C. J.; Lee, J.; Kim, Y.; Greco, T.; Ippen, C.; Wedel, A.; Ju, B. K.; et al. Transparent InP Quantum Dot Light-Emitting Diodes with ZrO2 Electron Transport Layer and Indium Zinc Oxide Top Electrode. *Adv. Funct. Mater.* **2016**, *26*, 3454−3461.
(87) Ji, W.; Lv, Y.; Jing, P.; Zhang, H.; Wang, J.; Zhang, H.; Zhao, J. Highly Efficient and Low Turn-On Voltage Quantum Dot Light-Emitting Diodes by Using a Stepwise Hole-Transport Layer. *ACS Appl. Mater. Interfaces* **2015**, *7*, 15955−15960.
(88) Jang, I.; Kim, J.; Ippen, C.; Greco, T.; Oh, M. S.; Lee, J.; Kim, W. K.; Wedel, A.; Han, C. J.; Park, S. K. Inverted InP Quantum Dot Light-Emitting Diodes Using Low-Temperature Solution-Processed Metal-Oxide as an Electron Transport Layer. *Jpn. J. Appl. Phys.* **2015**, *54*, 02BC01.
(89) Jang, I.; Kim, J.; Park, C. J.; Ippen, C.; Greco, T.; Oh, M. S.; Lee, J.; Kim, W. K.; Wedel, A.; Han, C. J.; et al. Study of Ethanolamine Surface Treatment on the Metal-Oxide Electron Transport Layer in Inverted InP Quantum Dot Light-Emitting Diodes. *Electron. Mater. Lett.* **2015**, *11*, 1066−1071.
(90) Wang, H. C.; Zhang, H.; Chen, H. Y.; Yeh, H. C.; Tseng, M. R.; Chung, R. J.; Chen, S.; Liu, R. S. Cadmium-Free InP/ZnSeS/ZnS Heterostructure-Based Quantum Dot Light-Emitting Diodes with a ZnMgO Electron Transport Layer and a Brightness of Over 10 000 Cd M−2. *Small* **2017**, *13*, 1603962.
(91) Wu, H.; Huang, F.; Mo, Y.; Yang, W.; Wang, D.; Peng, J.; Cao, Y. Efficient Electron Injection from a Bilayer Cathode Consisting of Aluminum and Alcohol-/Water-Soluble Conjugated Polymers. *Adv. Mater.* **2004**, *16*, 1826−1830.
(92) An, D.; Zou, J.; Wu, H.; Peng, J.; Yang, W.; Cao, Y. White Emission Polymer Light-Emitting Devices with Efficient Electron Injection from Alcohol/Water-Soluble Polymer/Al Bilayer Cathode. *Org. Electron.* **2009**, *10*, 299−304.
(93) He, Z.; Zhong, C.; Huang, X.; Wong, W. Y.; Wu, H.; Chen, L.; Su, S.; Cao, Y. Simultaneous Enhancement of Open-Circuit Voltage, Short-Circuit Current Density, and Fill Factor in Polymer Solar Cells. *Adv. Mater.* **2011**, *23*, 4636−4643.
(94) He, Z.; Zhong, C.; Su, S.; Xu, M.; Wu, H.; Cao, Y. Enhanced Power-Conversion Efficiency in Polymer Solar Cells Using an Inverted Device Structure. *Nat. Photonics* **2012**, *6*, 591−595.
(95) Zhang, K.; Zhong, C.; Liu, S.; Liang, A. H.; Dong, S.; Huang, F. High Efficiency Solution Processed Inverted White Organic Light Emitting Diodes with a Cross-Linkable Amino-Functionalized Polyfluorene as a Cathode Interlayer. *J. Mater. Chem. C* **2014**, *2*, 3270−3277.
(96) Stolz, S.; Lemmer, U.; Hernandez-Sosa, G.; Mankel, E. Correlation of Device Performance and Fermi Level Shift in the Emitting Layer of Organic Light-Emitting Diodes with Amine-Based Electron Injection Layers. *ACS Appl. Mater. Interfaces* **2018**, *10*, 8877−8884.
(97) Chen, L.; Wang, S.; Zhang, K.; Wang, A.; Fang, Y.; Du, Z. Enhanced Performances of Quantum Dot Light-Emitting Diodes with PFN-Adding Emitting Layer. *Org. Electron.* **2019**, *66*, 110−115.
(98) Jin, X.; Chang, C.; Zhao, W.; Huang, S.; Gu, X.; Zhang, Q.; Li, F.; Zhang, Y.; Li, Q. Balancing the Electron and Hole Transfer for

https://dx.doi.org/10.1021/acsenergylett.9b02824
ACS Energy Lett. 2020, 5, 1095−1106

Efficient Quantum Dot Light-Emitting Diodes by Employing a Versatile Organic Electron-Blocking Layer. *ACS Appl. Mater. Interfaces* **2018**, *10*, 15803−15811.
(99) Rahmati, M.; Dayneko, S.; Pahlevani, M.; Shi, Y. Highly Efficient Quantum Dot Light-Emitting Diodes by Inserting Multiple Poly(Methyl Methacrylate) as Electron-Blocking Layers. *Adv. Funct. Mater.* **2019**, *29*, 1906742.
(100) Gilot, J.; Barbu, I.; Wienk, M. M.; Janssen, R. A. J. The Use of ZnO as Optical Spacer in Polymer Solar Cells: Theoretical and Experimental Study. *Appl. Phys. Lett.* **2007**, *91*, 113520.
(101) Ma, Z.; Tang, Z.; Wang, E.; Andersson, M. R.; Inganäs, O.; Zhang, F. Influences of Surface Roughness of ZnO Electron Transport Layer on the Photovoltaic Performance of Organic Inverted Solar Cells. *J. Phys. Chem. C* **2012**, *116*, 24462−24468.
(102) You, J.; Chen, C. C.; Dou, L.; Murase, S.; Duan, H. S.; Hawks, S. A.; Xu, T.; Son, H. J.; Yu, L.; Li, G.; et al. Metal Oxide Nanoparticles as an Electron-Transport Layer in High-Performance and Stable Inverted Polymer Solar Cells. *Adv. Mater.* **2012**, *24*, 5267−5272.
(103) Adhikary, P.; Venkatesan, S.; Adhikari, N.; Maharjan, P. P.; Adebanjo, O.; Chen, J.; Qiao, Q. Enhanced Charge Transport and Photovoltaic Performance of PBDTTT-C-T/PC70BM Solar Cells via UV-Ozone Treatment. *Nanoscale* **2013**, *5*, 10007−10013.
(104) Wu, B.; Wu, Z.; Yang, Q.; Zhu, F.; Ng, T. W.; Lee, C. S.; Cheung, S. H.; So, S. K. Improvement of Charge Collection and Performance Reproducibility in Inverted Organic Solar Cells by Suppression of ZnO Subgap States. *ACS Appl. Mater. Interfaces* **2016**, *8*, 14717−14724.
(105) Ohtomo, A.; Kawasaki, M.; Koida, T.; Masubuchi, K.; Koinuma, H.; Sakurai, Y.; Yoshida, Y.; Yasuda, Y.; Segawa, Y. MgxZn1-XO as a II−VI Widegap Semiconductor Alloy. *Appl. Phys. Lett.* **1998**, *72*, 2466−2468.
(106) Tsukazaki, A.; Ohtomo, A.; Kita, T.; Ohno, Y.; Ohno, H.; Kawasaki, M. Quantum Hall Effect in Polar Oxide Heterostructures. *Science (Washington, DC, U. S.)* **2007**, *315*, 1388−1391.
(107) Janotti, A.; Van De Walle, C. G. Fundamentals of Zinc Oxide as a Semiconductor. *Rep. Prog. Phys.* **2009**, *72*, 126501.
(108) Womelsdorf, H.-H. Nanoparticulate, Redispersible Zinc Oxide Gels. U.S. Patent 6,710,091 B1, 2004.
(109) Chen, F.; Lv, P.; Li, X.; Deng, Z.; Teng, F.; Tang, A. Highly-Efficient and All-Solution-Processed Red-Emitting InP/ZnS-Based Quantum-Dot Light-Emitting Diodes Enabled by Compositional Engineering of Electron Transport Layers. *J. Mater. Chem. C* **2019**, *7*, 7636−7642.

https://dx.doi.org/10.1021/acsenergylett.9b02824
ACS Energy Lett. 2020, 5, 1095−1106